

## Spatial and Temporal Dynamics of Signalling Pathways

**Problem Presenter:** Rob Krams <sup>1</sup>

**Contributors:** Mike Baines, Bonhi Bhattacharya, Yohan Davit, Louise Dyson, Matthew Edgington, Sunny Modhara, Colin Please, Jennifer Siggers, Amy Smith and Marcus Tindall.

**November 4th 2011**

### 1 Introduction

In this report we present the findings of a problem presented to the Mathematics in Medicine Study Group of 2011, concerning the spatial and temporal dynamics of signalling pathways. This problem was motivated through cardiovascular disease (CVD), which describes the general class of disorders of the heart and blood circulatory system. CVD carries a high mortality with 4.3 million deaths in Europe and over 2.0 million deaths in the European Union (EU). CVD causes nearly half of all deaths in Europe (48%) with an estimated cost of 0.169 billion per annum. This makes CVD a considerable concern for health in Europe; innovations in this area will have significant repercussions both in terms of the human impact and the economic burden which treatment places on the EU.

Atherosclerosis, the accumulation of cholesterol deposits within plaques in arterial walls, is the underlying pathology of CVD related mortality. Its development is associated with varied risk factors (for example, hypercholesteraemia, hypertension and diabetes) all of which are associated with progression of the disease. These risk factors are important as they determine diagnostic developments and treatment of the disease. Remarkably, these risk factors predict a random or a homogeneous distribution of plaques over the arterial system, but this differs from clinical observations that indicate plaques are confined to curved vessels, bifurcations and side branches.

It has been postulated that disturbances of the blood flow pattern at these sites could induce atherosclerosis there, either through a direct effect on the endothelial cells or by remote transport effects (see, for example, Davies et al. (2005)). While early studies focused on the initiation of the disease, recent studies have strengthened the role of blood flow in advanced atherosclerosis by illustrating the role that blood flow plays in amongst others, advanced atherosclerotic disease (Chatzizisis et al., 2008), inflammation and plaque formation (Cheng et al., 2006). Despite strong evidence relating blood flow to all stages of atherosclerotic disease, however, the underlying mechanism linking shear stress to plaque formation is largely unknown and consequently a specific therapy is lacking.

Endothelial cells sense local blood flow by detecting the shear stress, although the mechanism by which they do this is not fully understood. Shear stress is the drag or frictional force exerted by the movement of blood with respect to the stationary endothelial layer. Due to the mechanical deformation of the endothelial cells by haemodynamic forces, several putative sensors are activated. After stimulation by shear stress activation of a combination of these receptors leads to the clustering of a series of membrane bound proteins which then activate down stream signalling pathways and eventually result in gene expression.

---

<sup>1</sup>email: r.krams@imperial.ac.uk

### 1.1 MAPK signalling cascade and KSR

One subset of signalling mechanisms which can be activated in this manner are the Mitogen Activated Protein Kinase (MAPK) pathways. MAPK cascades are evolutionarily conserved signalling pathways involved in the control of physiological and pathological intracellular processes. Each MAPK pathway contains a three tiered kinase cascade; the latter is sequentially activated by phosphorylation. The end product of this phosphorylation sequence, MAPK, can enter the nucleus and act as a transcription factor modulating gene expression (Aoki et al., 2011).

Activation of the MAPK pathway is dependent upon Ras, a member of a protein subfamily of small GTPases. Ras is ordinarily present attached to the cell membrane. Also located on the membrane is the inactive Raf kinase. Upon stimulation of the cell, for example, via shear stress, Ras and Raf associate to create a complex and allow the activation of Raf. This is thought to induce translocation of Kinase Suppressor of Ras (KSR) to the cell membrane.

KSR is a scaffold protein, a protein which provides a scaffold to coordinate the physical assembly of the components of a signalling network. KSR provides a scaffold that facilitates the phosphorylation reactions required for executing downstream signal transduction steps in the MAPK pathway (Nguyen et al., 2002). At the cell membrane KSR binds to the Ras-Raf complex and consequently initiates the MAPK cascade; this simplified representation is illustrated in Figure 1.1.

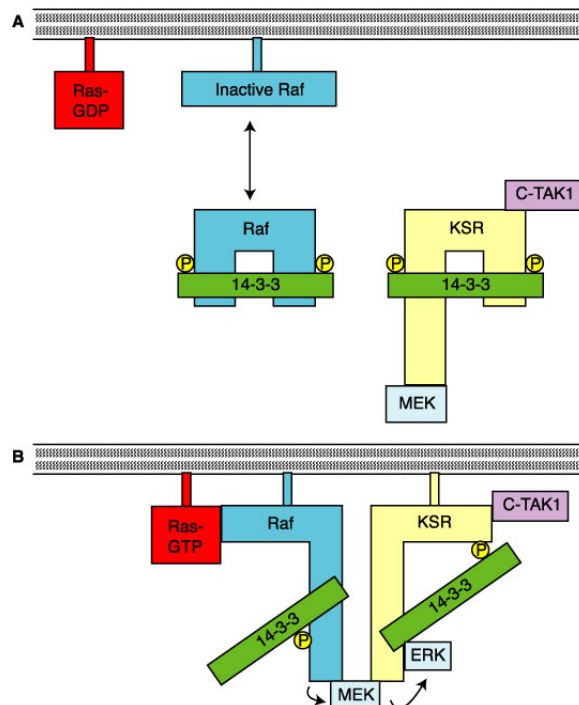


**Fig. 1.1:** Interaction of Ras, Raf and KSR to create the scaffold complex which allows initiation of the MAPK phosphorylation cascade. Figure taken from Raabe and Rapp (2002)

## 1.2 Cellular Movement and Intracellular crowding

However, for this process to occur, KSR must diffuse through the cytoplasm to reach the cell membrane. Although cell cytoplasm appears to be an unstructured, aqueous liquid, it is in fact structured on many length scales, from organelles like the mitochondria, endosomes, and the Golgi apparatus, to smaller scales such as the endoplasmic reticulum. This results in a higher order structure of the cytoplasm and as a consequence, diffusional movement of particles, such as macromolecules, can be obstructed.

Previous mathematical modelling of the MAPK signalling pathway has normally assumed that spatial effects can be neglected, and that the transport of KSR can be described using a system of coupled ordinary differential equations. This approximation is based on the idea that the characteristic times associated with the spatial transport mechanisms, for example, diffusion, are much smaller than those associated with reaction processes. This is generally true for small molecules, which are easily transported from the extracellular membrane to the nucleus, and are little affected by the presence of large intracellular structures within the cytoplasm.

These structures may have a profound effect upon the diffusion of large proteins, such as MAPK and KSR. Steric hindrance, binding and hydrodynamic interactions may significantly modify the transport kinetics, resulting in situations for which spatial gradients must be considered. For example, steric hindrance will increase the path length of the molecule, by making it more tortuous.

## 2 Mathematical Modelling

In this section we present a mathematical model of the processes involved in MAPK cascade activation with specific focus on the Ras-Raf-KSR activation process, and the contribution which diffusion makes to this process.

### 2.1 Apparent Diffusion Coefficient

We note that the interior of a cell is a highly crowded environment, so that the usual assumptions for diffusion may not be realistic. However, we can derive the usual diffusion equation by assuming there to be a particular fraction of the cell that consists of obstacles. We consider a population of individual molecules on a lattice (see Figure 2.1, moving in a random direction with rate  $\alpha$  per unit time and allow at most one molecule at any lattice point. If  $C_{i,j}(t)$  is the probability that a molecule is at grid point  $(i, j)$  at time  $t$ , and  $\phi$  is the fraction of space that is unoccupied, then

$$\begin{aligned}
 C_{i,j}(t + \Delta t) = & P(\text{molecule is at } (i, j) \text{ at time } t \text{ and that molecule remained in position}) \\
 & + P(\text{no molecule at } (i, j)) \cdot \{P(\text{molecule at } (i + 1, j) \text{ at } t \text{ and moved to } (i, j)) \\
 & + P(\text{molecule at } (i - 1, j) \text{ at } t \text{ and moved to } (i, j)) \\
 & + P(\text{molecule at } (i, j + 1) \text{ at } t \text{ and moved to } (i, j)) \\
 & + P(\text{molecule at } (i, j - 1) \text{ at } t \text{ and moved to } (i, j))\}.
 \end{aligned} \tag{2.1}$$

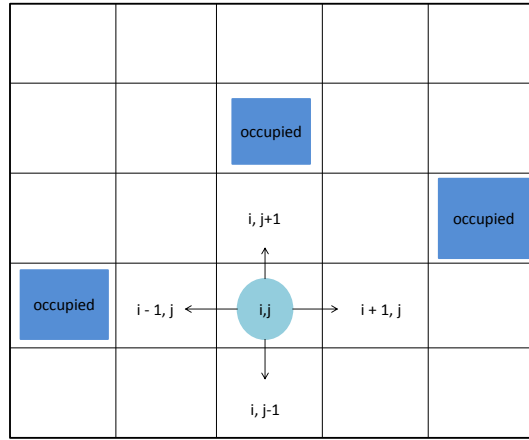


**Fig. 2.1:** Depiction of the cell as a lattice. The molecule can move in one of four directions from its position, and only one molecule may be in a given grid square at any time. The movement of the molecule is impeded by other molecules which occupy certain lattice squares; these occupied squares are assumed to be so for all time.

Thus we have that

$$C_{i,j}(t + \Delta t) = C_{i,j}(t) \left( 1 - \alpha\phi\Delta t + \frac{\alpha\Delta t\phi}{4} (C_{i+1,j}(t) + C_{i-1,j}(t) + C_{i,j+1}(t) + C_{i,j-1}(t)) \right) + \frac{\alpha\Delta t\phi}{4} (1 - C_{i,j}(t)) (C_{i-1,j}(t) + C_{i+1,j}(t) + C_{i,j+1}(t) + C_{i,j-1}(t)), \quad (2.2)$$

from which we find

$$\frac{C_{i,j}(t + \Delta t) - C_{i,j}(t)}{\Delta t} = \frac{\alpha\phi\delta^2}{4} \left( \frac{C_{i+1,j}(t) - 2C_{i,j}(t) + C_{i-1,j}(t)}{\delta^2} + \frac{C_{i,j+1}(t) - 2C_{i,j}(t) + C_{i,j-1}(t)}{\delta^2} \right). \quad (2.3)$$

Therefore we have

$$\frac{\partial C}{\partial t} = \left( \lim_{\Delta t, \delta \rightarrow 0} \frac{\alpha\phi\delta^2}{4} \right) \nabla^2 C, \quad (2.4)$$

where  $\delta$  is the lattice step size and we assume that  $\alpha$  scales so that

$$D_A = \left( \lim_{\Delta t, \delta \rightarrow 0} \alpha\phi\delta^2/4 \right),$$

is finite. We can see that this is the Fickian diffusion equation, where we have an apparent diffusion coefficient,  $D_A$ , which is related to the Fickian diffusion coefficient,  $D$ , by  $D_A = \phi D$ .

Note that this depends upon the assumption that the probability of a cell being stopped by an occupied space remains constant throughout time and throughout space, and as the lattice grid size decreases. However, not all molecules responsible for cellular crowding are fixed to certain positions within cells and in an intracellular environment occupation of a certain space does not necessarily correlate with complete blocking of movement into that area. Some molecules, for example, may be able to squeeze past others. In this case the probability that the molecules being considered will be at given points in space at certain moments of time

can no longer be considered as constant and hence, cannot be modelled by the diffusion equation based on classical Fickian laws.

Molecular crowding is thought to affect solute diffusion by increasing the effective viscosity of the medium (Zimmerman and Minton, 1993). In fact crowding seems to contribute significantly to the high viscosity of the cytoplasm which Verkman (2002) determined to be three to fourfold higher than that of water. These observations suggest we may consider that diffusion in the cell cytoplasm and nucleus is anomalous.

Anomalous diffusion, in which mean squared displacement does not increase linearly with time, has previously been indicated in solute diffusion in media crowded with obstacles, both fixed or mobile, or in the case when diffusion rates are affected by, for example, active transport processes (Weiss et al., 2004; Guigas and Weiss, 2008; Banks and Fradin, 2005). However, there is experimental evidence to show that solute diffusion in solutions and cellular aqueous compartments is generally a consequence of Brownian diffusion. Conversely, in cell membranes, both Brownian and anomalous diffusion have been observed (Dix and Verkman, 2008; Feder et al., 1996).

The delay effect due to intracellular crowding has also been explored theoretically by Novak et al. (2009), who used a porous medium approach, based on a homogenization technique, to study the effect of the intracellular structures upon the effective diffusion. Their main idea is to treat large proteins as point particles, by fictitiously modifying the size of the obstacles, i.e., making them larger. They show that the excluded volume effect alone can account for a four-to-sixfold reduction in diffusive transport in cells, therefore suggesting that spatial effects must be taken into account for the MAPK signalling pathway.

Although the work in Novak et al. (2009) provides a significant insight into the mechanisms that influence proteins transport within the cytoplasm, there are a number of hypotheses that require careful consideration. *A priori*, it is unclear if a notion of Fickian effective diffusion is even relevant. For instance, short time phenomena, or binding of the protein to the intracellular structure, may lead to anomalous effects.

For the purposes of this study, and as a first attempt to consider spatial effects for modelling the MAPK signalling pathway, we hypothesize that the transport of MAPK and KSR can be described in terms of simple Fickian effective diffusion equations.

## 2.2 Mathematical Model of KSR Diffusion and Receptor Interaction

In this section we formulate equations and boundary conditions for a simplified model of the process of MAPK production described in Section 1.1. This process has been simplified as illustrated in Figure 2.2, in which we aim to incorporate all the steps that have a significant effect on the rate of production. We assume that Raf acts as an inactive receptor,  $I$ , present on the cell membrane. Upon sensing some kind of signal (for example, shear stress) this receptor becomes activated,  $A$ . (This is analogous to the biological association of Ras and Raf creating an active complex as described in Section 1.1).

This activation induces molecules of KSR,  $K$ , to diffuse through the cytoplasm until they reach the membrane whereupon they bind to an active receptor creating a bound complex,  $B$ . This complex is capable of producing activated MAPK,  $M$ . Note that in simplifying this model, we have subsumed the phosphorylation cascade

that creates activated MAPK into a single step. Initially we consider a one-dimensional model of the cell with the cell membrane at  $x = 0$  and the nucleus at  $x = L$ .

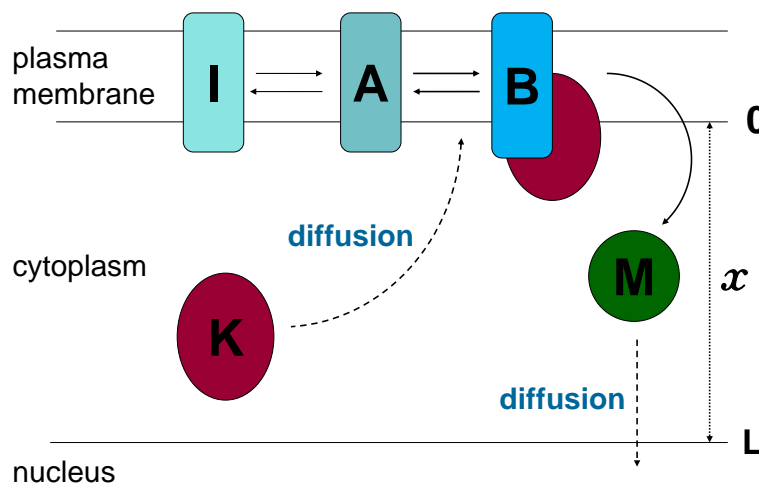


**Fig. 2.2:** Simplified model of MAPK production. At the plasma membrane inactive receptors  $I$  can be activated,  $A$ . This induces KSR,  $K$ , to diffuse through the cytoplasm and when it reaches the membrane it binds with the active receptor to form a complex,  $B$ , which consequently produces activated MAPK,  $M$ .

The variables appearing in the model are listed in Table 1. Also listed in this table are the parameters of the model which describe the rate constants and diffusion coefficients.

Symbol	Description	Dimensions
$L$	Distance from nucleus to cell membrane	$L$
$c_K$	Concentration of KSR in the cytoplasm	$L^{-3}$
$c_M$	Concentration of MAPK in the cytoplasm	$L^{-3}$
$c_I$	Concentration of inactive receptors on the membrane	$L^{-2}$
$c_A$	Concentration of active, unbound receptors on the membrane	$L^{-2}$
$c_B$	Concentration of active, bound receptors on the membrane	$L^{-2}$
$D_K$	Effective diffusion coefficient of KSR in cytoplasm	$L^2 T^{-1}$
$D_M$	Effective diffusion coefficient of MAPK in cytoplasm	$L^2 T^{-1}$
$k_1$	Rate of receptor activation	$T^{-1}$
$k_2$	Rate of receptor deactivation	$T^{-1}$
$\hat{k}_1$	Rate of KSR binding to receptor	$L^3 T^{-1}$
$\hat{k}_2$	Rate of KSR unbinding to receptor	$T^{-1}$
$k_M$	Rate of production of MAPK per unit concentration of bound receptor	$T^{-1}$

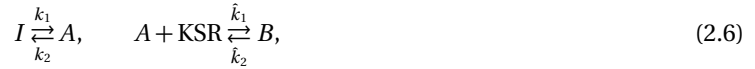
**Table 1:** Dependent variables and parameters appearing in the governing equations and boundary conditions of the KSR diffusion model.

**In the cytoplasm** ( $0 \leq x \leq L$ ) We only consider the concentrations of KSR,  $c_K(x, t)$ , and MAPK,  $c_M(x, t)$ . Following the discussion in Section 2.1, we assume that both the KSR and MAPK molecules obey a Fickian diffusion process with effective diffusion coefficients  $D_K$  and  $D_M$  respectively, meaning the typical distance travelled by a molecule scales with the square root of the time. Thus

$$\frac{\partial c_K}{\partial t} = D_K \frac{\partial^2 c_K}{\partial x^2}, \quad \frac{\partial c_M}{\partial t} = D_M \frac{\partial^2 c_M}{\partial x^2}, \quad (2.5)$$

where  $t$  is time.

**At the cell membrane** ( $x = 0$ ) We assume that, immediately the cell is activated, the following reactions occur:



where  $I$  is an inactive receptor,  $A$  is an active receptor and  $B$  is the bound complex of a KSR molecule on an active receptor; these have concentrations  $c_I(t)$ ,  $c_A(t)$ ,  $c_B(t)$ , respectively. Assuming the reaction rates are based on the stoichiometric rate constants leads to the following equations governing the concentrations at  $x = 0$ :

$$\frac{dc_I}{dt} = k_2 c_A - k_1 c_I, \quad (2.7)$$

$$\frac{dc_A}{dt} = k_1 c_I - k_2 c_A + \hat{k}_2 c_B - \hat{k}_1 c_A c_K, \quad (2.8)$$

$$\frac{dc_B}{dt} = \hat{k}_1 c_A c_K - \hat{k}_2 c_B, \quad (2.9)$$

$$D_K \frac{\partial c_K}{\partial x} = \frac{dc_B}{dt}, \quad (2.10)$$

$$D_M \frac{\partial c_M}{\partial x} = -k_M c_B. \quad (2.11)$$

The last two of the above equations follow from the fact that their left-hand sides are the Fickian fluxes of, respectively, KSR and MAPK from the cytoplasm the membrane, and the assumption that a bound KSR–receptor complex produces a constant flux  $k_M$  per unit bound receptor concentration.

**At the nucleus** ( $x = L$ ) We assume that KSR molecules cannot enter the nucleus and that MAPK is immediately absorbed (this assumption may need changing when we refine the model). This leads to the boundary conditions

$$-D_K \frac{\partial c_K}{\partial x} = 0, \quad c_M = 0. \quad (2.12)$$

**Initial conditions** ( $t = 0$ ) We assume that initially all receptors are inactive (and therefore unbound) and that, immediately after activation, all KSR is released into the cytoplasm with a uniform concentration. Thus

$$c_I = N, \quad c_A = c_B = 0, \quad c_K = c_0, \quad c_M = 0. \quad (2.13)$$

**Important relationships** Note that both the total concentration of receptors and the total number of KSR molecules in the system do not change in time. For the receptors we prove this mathematically by adding

(2.7), (2.8) and (2.9) to give

$$\frac{d}{dt}(c_I + c_A + c_B) = 0,$$

and thus the sum of the receptor concentrations does not change in time. The initial conditions imply that the relationship

$$c_I + c_A + c_B = N \tag{2.14}$$

is always obeyed. For KSR we integrate (2.5a) over  $0 \leq x \leq L$  to give

$$\frac{d}{dt} \left( \int_0^L c_K dx \right) = D_K \left[ \frac{\partial c_K}{\partial x} \right]_{x=0}^L = -\frac{dc_B}{dt}$$

where the second equality arises from applying the boundary conditions (2.10) and (2.12a). This equation shows that the number of moles of KSR per unit surface area (both that bound to the surface and that in the cytoplasm) does not change in time. Integrating and applying the boundary conditions we obtain the relationship

$$c_B + \int_0^L c_K dx = Lc_0. \tag{2.15}$$

### 2.2.1 Steady state solution

In this section we find a steady solution of the governing equations that were formulated in Section 2.2. Assuming a steady solution, equations (2.5) subject to the boundary conditions at the nucleus (2.12) have the solution that  $c_K$  is spatially constant and  $c_M = C(L - x)$  for some constant of integration  $C$ .

The boundary conditions (2.7)–(2.11) give

$$c_A = \frac{k_1}{k_2} c_I, \tag{2.16}$$

$$c_B = \frac{\hat{k}_1}{\hat{k}_2} c_K c_A = \frac{k_1 \hat{k}_1}{k_2 \hat{k}_2} c_K c_I, \tag{2.17}$$

$$D_M C = k_M c_B \Rightarrow C = \frac{k_M}{D} \frac{k_1 \hat{k}_1}{k_2 \hat{k}_2} c_K c_I, \tag{2.18}$$

Eliminating  $c_A$ ,  $c_B$  and  $C$  from the conservation equations (2.14) and (2.15) gives

$$\left( 1 + \frac{k_1}{k_2} + \frac{k_1 \hat{k}_1}{k_2 \hat{k}_2} c_K \right) c_I = N, \quad \frac{k_1 \hat{k}_1}{k_2 \hat{k}_2} c_K c_I + Lc_K = Lc_0. \tag{2.19}$$

Eliminating  $c_I$  from these equations and solving for  $c_K$  gives

$$c_K = \frac{1}{2} \left[ -\left( \frac{N}{L} - c_0 + X \right) \pm \sqrt{\left( \frac{N}{L} - c_0 + X \right)^2 + 4Xc_0} \right],$$

where

$$X = \frac{k_2 \hat{k}_2}{k_1 \hat{k}_1} \left( 1 + \frac{k_1}{k_2} \right). \quad (2.20)$$

Requiring  $c_K$  to be positive for physical reasons,

$$c_K = \frac{1}{2} \left[ \sqrt{\left( \frac{N}{L} - c_0 + X \right)^2 + 4Xc_0} - \left( \frac{N}{L} - c_0 + X \right) \right], \quad (2.21)$$

from which  $c_I$  can be found by rearranging (2.19a) and  $c_A$ ,  $c_B$  and  $C$  can then be found from (2.16)–(2.18).

### 2.2.2 Non-dimensional equations

We define  $t = t^*T$ ,  $c_I = c_I^*C_I$ ,  $c_A = c_A^*C_A$ ,  $c_k = c_k^*C_k$ ,  $c_M = c_M^*C_M$ ,  $x = x^*L$  where  $T$  is a typical, yet to be determined timescale,  $C_I$ ,  $C_A$ ,  $C_k$  and  $C_M$  are typical concentrations, which are also yet to be determined, and  $L$  is the typical lengthscale. Starred variables indicate dimensionless quantities and non-starred variables represent dimensional quantities. We substitute these into the equations formulated in Section 2.2, boundary conditions and initial conditions, whilst at the same time omitting the star on the dimensionless variables to give the following non-dimensional system in which the timescale and concentration scales are yet to be determined:

$$\text{Concentration of KSR } C_k: \quad \frac{\partial c_k}{\partial t} = \frac{D_k T}{L^2} \frac{\partial^2 c_k}{\partial x^2}, \quad (2.22a)$$

$$\text{Concentration of MAPK } C_M: \quad \frac{\partial c_M}{\partial t} = \frac{D_M T}{L^2} \frac{\partial^2 c_M}{\partial x^2}. \quad (2.22b)$$

**At the cell membrane ( $x = 0$ )**

$$\text{Inactive receptor } c_I: \quad \frac{dc_I}{dt} = \frac{TC_A}{C_I} k_2 c_A - T k_1 c_I, \quad (2.23a)$$

$$\text{Active receptor } c_A: \quad \frac{dc_A}{dt} = -T k_2 c_A + \frac{TC_I}{C_A} k_1 c_I - TC_k \hat{k}_1 c_A c_k + \frac{TC_B}{C_A} \hat{k}_2 c_B, \quad (2.23b)$$

$$\text{Bound receptor } c_B: \quad \frac{dc_B}{dt} = \frac{TC_A C_K}{C_B} \hat{k}_1 c_A c_k - T \hat{k}_2 c_B, \quad (2.23c)$$

$$\text{Conservation: } C_B c_B + C_A c_A + C_I c_I = N, \quad (2.23d)$$

$$\text{Flux of KSR: } \frac{\partial c_k}{\partial x} = \frac{LC_B}{TD_k C_k} \frac{dc_B}{dt}, \quad (2.23e)$$

$$\text{Flux of MAPK: } \frac{\partial c_M}{\partial x} = \frac{Lk_M C_B}{D_M C_M} c_B. \quad (2.23f)$$

**At the nucleus ( $x = L$ )**

$$\text{KSR: } \frac{C_k}{L} \frac{\partial c_k}{\partial x} = 0, \quad (2.24a)$$

$$\text{MAPK: } C_M c_M = 0. \quad (2.24b)$$

**Initial conditions (t = 0)**

$$c_I = \frac{N}{C_I}, \quad c_A = c_B = c_M = 0, \quad c_k = \frac{c_0}{C_k}. \quad (2.25)$$

**Scaling choices** We non-dimensionalise the active, bound and inactive receptor concentrations on the initial receptor concentration i.e.

$$C_B = C_A = C_I = N,$$

so that the boundary condition (2.23d) now gives

$$c_A + c_B + c_I = 1. \quad (2.26)$$

Receptors are thus conserved since the sum of the receptor concentrations does not change in time:

$$\frac{d}{dt}(c_A + c_B + c_I) = 0. \quad (2.27)$$

We non-dimensionalise the concentration of KSR on its initial concentration,  $c_0$ . Since  $c_M$  only appears in (2.23f), we choose to normalise the parameter grouping in this equation. Thus we obtain the scale

$$C_M = \frac{k_M LN}{D_M}.$$

Choosing an appropriate timescale is not so obvious and will largely depend on the intrinsic processes of the system which are most important. These include receptor dynamics, the production of MAPK or indeed the diffusive properties of MAPK and KSR. Deciding which of these processes is the most important involves close examination of the parameter values and identification of the dominant coefficients in the governing equations. Follow up work will determine the important timescales and hence identify the best choices for non-dimensionalisation. Here, our final non-dimensional equations retain the yet to be determined timescale  $T$ .

$$\text{Concentration of KSR } C_k: \quad \frac{\partial c_k}{\partial t} = \frac{D_k T}{L^2} \frac{\partial^2 c_k}{\partial x^2}, \quad (2.28a)$$

$$\text{Concentration of MAPK } C_M: \quad \frac{\partial c_M}{\partial t} = \frac{D_M T}{L^2} \frac{\partial^2 c_M}{\partial x^2}. \quad (2.28b)$$

**At the cell membrane (x = 0)**

$$\text{Inactive receptor } c_I: \quad \frac{dc_I}{dt} = T k_2 c_A - T k_1 c_I, \quad (2.29a)$$

$$\text{Active receptor } c_A: \quad \frac{dc_A}{dt} = -T k_2 c_A + T k_1 c_I - T c_0 \hat{k}_1 c_A c_k + T \hat{k}_2 c_B, \quad (2.29b)$$

$$\text{Bound receptor } c_B: \quad \frac{dc_B}{dt} = T c_0 \hat{k}_1 c_A c_k - T \hat{k}_2 c_B, \quad (2.29c)$$

$$\text{Conservation of receptor: } c_B + c_A + c_I = 1, \quad (2.29d)$$

$$\text{Flux of KSR: } \frac{\partial c_k}{\partial x} = \frac{LN}{T D_k c_0} \frac{dc_B}{dt}, \quad (2.29e)$$

$$\text{Flux of MAPK: } \frac{\partial c_M}{\partial dx} = c_B. \quad (2.29f)$$

At the nucleus ( $x = L$ )

$$\text{KSR: } \frac{c_0}{L} \frac{\partial c_k}{\partial x} = 0, \Rightarrow \frac{\partial c_k}{\partial x} = 0. \tag{2.30a}$$

$$\text{MAPK: } \frac{k_M LN}{D_M} c_M = 0, \Rightarrow c_M = 0. \tag{2.30b}$$

Initial conditions ( $t = 0$ )

$$c_I = 1, \quad c_A = c_B = c_M = 0, \quad c_k = 1. \tag{2.31}$$

We may find that diffusion of KSR is the rate-limiting process and hence the most important. We would then choose a timescale by normalising the parameter grouping in (2.28a). A similar normalisation of the parameter grouping in equation (2.28b) could be carried out when the diffusivity of MAPK is deemed important. In the case where receptor dynamics are important, normalisation of the parameter groupings in the boundary conditions would define an appropriate timescale. For the reasons detailed above, initial simulations of the model will be carried out using the dimensional system of equations from Section 2.2.

### 2.2.3 Parameter Values

Parameter values that we were able to source from the literature are detailed in Table 2 together with references of the papers they were sourced from. Further discussion of the parameter values may be found in Section 4.

Parameter	Description	Value	Notes	Reference
$D_K$	KSR diffusion coefficient			
$D_M$	wildtype MAPK diffusion coefficient	$7.7 \pm 0.4 \mu\text{m}^2/\text{s}$	no serum	Lidke et al. (2010)
		$6.6 \pm 0.3 \mu\text{m}^2/\text{s}$	with serum	Lidke et al. (2010)
$C_M$	MAPK expression levels	$0.82 \pm 0.4 \mu\text{M}$	in cytoplasm	Lidke et al. (2010)
		$0.77 \pm 0.2 \mu\text{M}$	in nucleus	Lidke et al. (2010)
$C_K$	KSR expression levels			
$k_1$	rate of activation of receptors	$2\text{s}^{-1}$		Hibino et al. (2011)
$k_2$	rate of deactivation of receptors	$3.7\text{s}^{-1}$		Hibino et al. (2011)
$k_M$	rate of production of MAPK from the complex	$1/180\text{s}^{-1}$		Lidke et al. (2010)
$\hat{k}_1$	rate of KSR binding to receptor			
$\hat{k}_2$	rate of KSR unbinding to receptor			
$C_{I_0}$	concentration of receptors	60,000 per cell		Philips et al. (2008)
		of $5\mu\text{m}$ radius		
	time for the concentration of MAPK, $c_M$ to reach steady state	$\sim 300\text{s}$		Lidke et al. (2010)

**Table 2:** Parameters appearing in the governing equations and boundary conditions of the KSR diffusion model and their values.

### 3 Model Results

#### 3.1 One Dimension

The equations are solved first in one dimension, using the Numerical Algorithms Group solver d03pl (NAG). This routine integrates a system of linear or nonlinear convection-diffusion equations with coupled ordinary differential equations (ODEs). The method of lines is used to reduce the partial differential equations to a system of ODEs, which are then solved using a backwards differentiation formula (BDF) method.

Since we have not been able to find biologically reasonable parameter values for all our parameters, and do not have orders of magnitude approximations for the others, we will simulate the system with demonstrative parameters detailed in Table 3. This enables us to gain knowledge of the system as a whole, before determining all the parameter values. We assume for the simulations that  $L = 5\mu m$ , and take initial conditions  $I = 2.5$ ,  $A = B = 0$ .

Parameter	Description	Value
$D_K$	KSR diffusion coefficient	1
$D_M$	MAPK diffusion coefficient	1
$C_M(x, 0)$	MAPK expression levels	0
$C_K(x, 0)$	KSR expression levels	1
$k_1$	rate of activation of receptors	2
$k_2$	rate of deactivation of receptors	3.7
$k_M$	rate of production of MAPK from the complex	0.1
$\hat{k}_1$	rate of KSR binding to receptor	3
$\hat{k}_2$	rate of KSR unbinding to receptor	3

**Table 3:** Demonstrative parameters used for simulation purposes.

Our numerical results are shown in Figure 3.2 and 3.3, progressing in time from the top to the bottom. The solutions to the ODEs is shown in Figure 3.1. Initially all the receptors are inactive and unbound ( $C_I$ ), and the KSR ( $C_k$ ) is at a constant concentration in the cytoplasm with no MAPK ( $C_M$ ). When we begin the simulation, the receptors start to become active ( $C_A$ ) so that  $C_I$  decreases and  $C_A$  increases.

As the active receptors are then bound by the KSR, the bound complex concentration,  $C_B$ , rises and starts to produce MAPK. This can then be seen in the spatial solutions, as the MAPK starts to diffuse across the domain. We can see from Figure 3.1 that the boundary ODEs reach a steady state very quickly and the spatially dependent variables go more slowly towards their steady state solutions, with KSR constant and MAPK linearly decreasing across the domain. This compares well with our predictions for the steady state solutions (see Section 2.2.1).

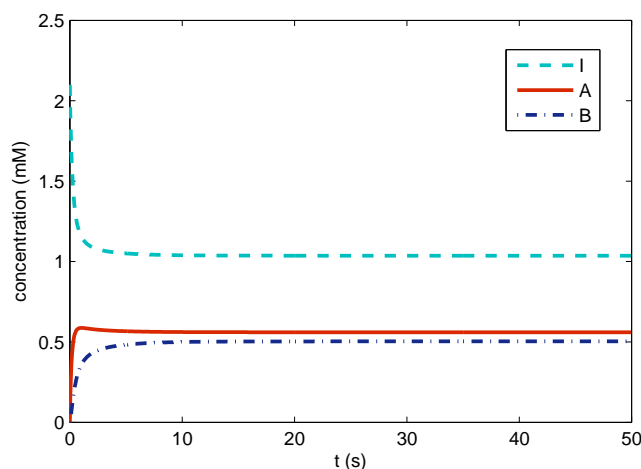


**Fig. 3.1:** Simulation of the model in 1D, showing the concentration of active (*A*), inactive (*I*) and bound (*B*) receptors at the boundary as time increases.

### 3.2 Two Dimensions

In order to explore more realistic geometries, we used COMSOL Multiphysics to solve the system of differential equations on a 2-D cell. To facilitate implementation, we slightly modified the problem presented in section Section 2.2, and treated the extracellular membrane as an independent phase, rather than a boundary. The results are illustrated Figure 3.4 for the initial MAPK concentration fields, and the steady-state solution. Future modelling work should focus on developing a full 3-D model, in which gradients of concentrations along the extracellular membrane can be considered, in order to take into account the spatial variability of the shear stress activation.

## 4 Conclusions and Further Work

Signal transduction pathways such as the MAPK cascade are complex. In addition to the reactions involved in activating the KSR-Ras-Raf complex to initiate the cascade, there are the phosphorylation steps involved in releasing activated MAPK molecules which can influence transcription. These reactions are further complicated by the necessity of KSR and MAPK to diffuse within the crowded medium of the cytoplasm in order to reach the cellular locations where they may have an effect. By considering reactions between relevant molecules and receptors at the cell membrane, and diffusion of these molecules towards the membrane, we have created a preliminary model to describe the processes involved in the MAPK pathway.

The ultimate aim of this work is to extend existing models by including the spatial dependence of the concentration of KSR and MAPK within the cytoplasm. We have presented a simple but insightful model which, to our knowledge, is the first to include the effect of diffusion in the study of mechano-transduction dynamics and thus represents a significant new approach to this problem, laying the foundations for further work. The potential for extending this project is vast.

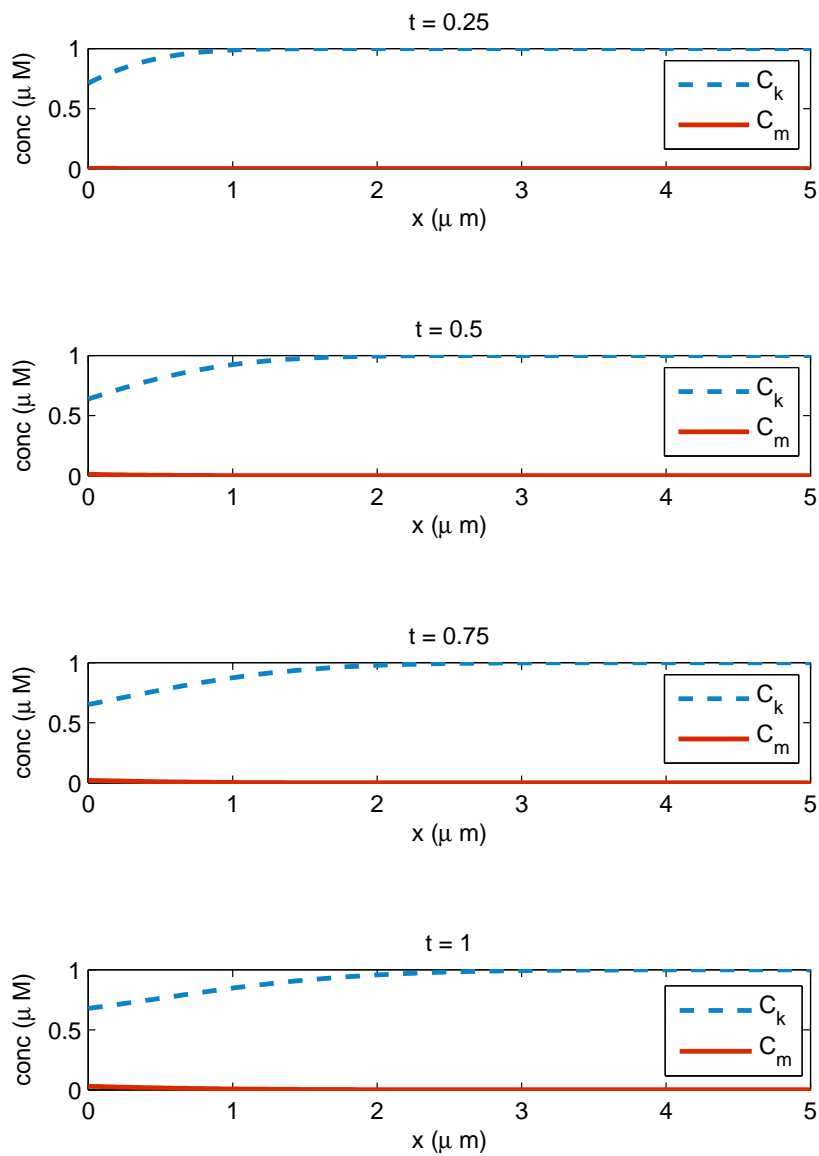


**Fig. 3.2:** Simulation of the model in 1D at short times as the boundary conditions quickly go to steady state.

Validating our model has been hindered by an absence of parameter values. This lack of parameter values stems from the fact that in creating a mathematical model, we consider reactions which are represented as equations. In doing this we derive, for example, rate parameters and binding coefficients, which are not necessarily meaningful in a biological sense. Hence, they may not have been measured or may not be measur-

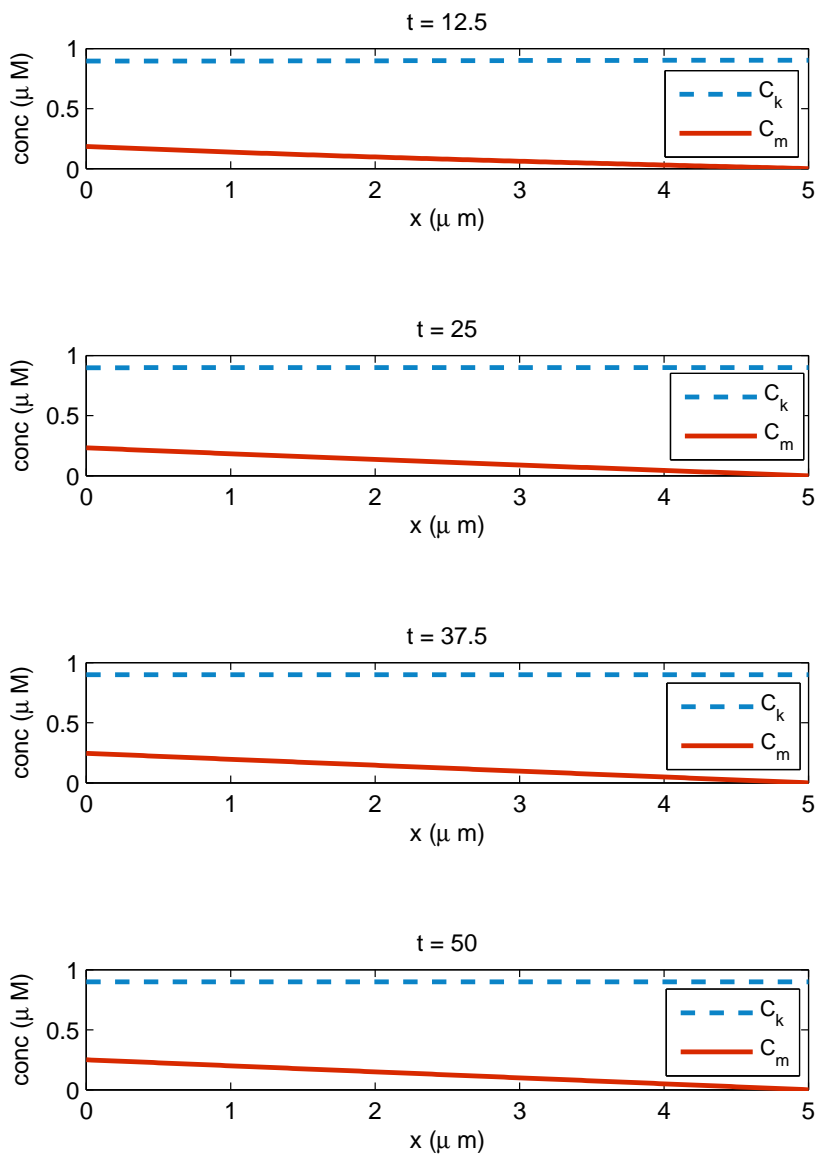


**Fig. 3.3:** Simulation of the model in 1D at long times as the KSR and MAPK reach a steady state within the domain.

able. Another issue we face is that the parameter values we may collect can often come from a variety of cell types or experimental conditions. In the short term, the next step that we can take is to conduct a thorough literature search for the relevant parameter ranges. In the longer term, we may use our mathematical efforts to outline key parameter values necessary for modelling purposes. In this way we may guide experimentalists

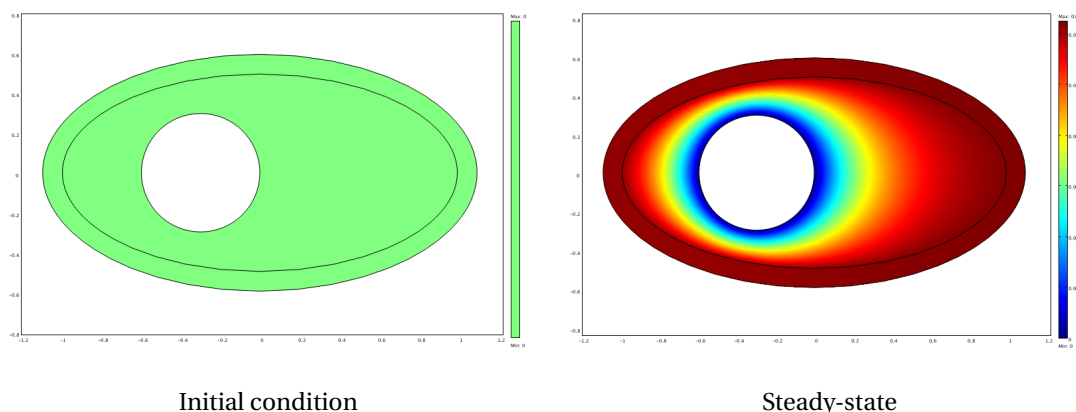


**Fig. 3.4:** Illustration of the MAPK concentration field within a two-dimensional cell.

by highlighting which measurements would most benefit model simulation and validation.

We now outline some potential research directions which could follow from our initial investigations.

Our model represents a highly simplified version of the actual physiology found *in vivo*. In future, we hope to formulate a more sophisticated model for the description of the MAPK pathways. In particular, the pathway initiated by the binding of active receptor and KSR, which eventually triggers the release of MAPK, is in reality far more complex than we have described in our equations. The phosphorylation reactions which comprise this pathway can engender significant delays which will affect the results of the model. In particular it may well affect the dynamic behaviour we observe. To rectify this we can include time delays into the reactions and into the diffusive processes. Alternatively we may choose to incorporate the phosphorylation steps (and thus enzymatic processes) into the model for which information from existing models (see, for example, Qiao et al. (2007)) could be utilised.

As previously discussed in Section 2.1, the cytoplasm in cells is far from a Newtonian fluid: in fact, it is an environment packed with relatively large intracellular structures, which are hypothesized to have a significant influence upon the diffusion of MAPK and KSR. In this report, we assumed Fickian diffusion of both proteins. Given available experimental data, we could capture cell crowding via a suitable reduction in the effective diffusion coefficient. Another approach might be to explicitly calculate an effective diffusivity coefficient by applying homogenisation or volume averaging methods. This would require some knowledge of the geometry of the structures within the cytoplasm, which could be obtained from high-resolution medical imaging. However, in the future we aim to address the non-Fickian diffusion of the proteins within a crowded environment, by applying the theory of anomalous diffusion.

One final aspect which we have not yet considered is the direct link between shear stress on the endothelial wall and the activation of receptors on the membrane. This would involve a study of the mechanisms by which shear stress is sensed, and could provide the key relation between blood flow in vessels and the induction of gene transcription in the nuclei of cells. We would in this case, consider more rigorously, reactions occurring at the cell membrane; currently our model has a simplified version of the receptor activation process needed to initiate the MAPK cascade and is decoupled from the shear stress sensor signals.

Furthermore, since the completion of this study group we have become aware of the observation that the inhibition of KSR has no effect on the dynamics of the MAPK. It has been proposed that a direct effect of crowding is affecting the dynamics. Essentially it is assumed that the proteins diffuse minimally and thereby stay in a confined space where they interact possibly negating the need of diffusing to the membrane for activation. This is an issue that we will research more thoroughly in follow up work.

We believe that the work of this study group has created the foundations of a model which may be elaborated with a greater dependence on the underlying biology in order to create a model of the MAPK signalling pathway, which includes both spatial and temporal organisation.

## References

- K. Aoki, M. Yamada, K. Kunida, S. Yasuda, and M. Matsuda. Processive phosphorylation of erk map kinase in mammalian cells. *108(31):12675–12680*, 2011.
- D. S. Banks and C. Fradin. Anomalous diffusion of proteins due to molecular crowding. *Biophysical Journal*, 89(5):2960 – 2971, 2005.
- Y. S. Chatzizisis, M. Jonas, A. U. Coskun, R. Beigel, B. V. Stone, C. Maynard, R. G. Gerrity, W. Daley, C. Rogers, E. R. Edelman, C. L. Feldman, and P. H. Stone. Prediction of the localization of high-risk coronary atherosclerotic plaques on the basis of low endothelial shear stress. *Circulation*, 117(8):993–1002, 2008.
- C. Cheng, D. Tempel, R. van Haperen, A. van der Baan, F. Grosveld, M. J. Daemen, R. Krams, and R. de Crom. Atherosclerotic lesion size and vulnerability are determined by patterns of fluid shear stress. *Circulation*, 113(23):2744–2753, 2006.
- P. Davies, J. Spaan, and R. Krams. Shear stress biology of the endothelium. *Annals of Biomedical Engineering*, 33:1714–1718, 2005.
- J. A. Dix and A. Verkman. Crowding effects on diffusion in solutions and cells. *Annual Review of Biophysics*, 37(1):247–263, 2008.
- T. Feder, I. Brust-Mascher, J. Slattery, B. Baird, and W. Webb. Constrained diffusion or immobile fraction on cell surfaces: a new interpretation. *Biophysical Journal*, 70(6):2767 – 2773, 1996.
- G. Guigas and M. Weiss. Sampling the cell with anomalous diffusion - the discovery of slowness. *Biophysical Journal*, 94(1):90 – 94, 2008.
- K. Hibino, T. Shibata, T. Yanagida, and Y. Sako. Activation kinetics of raf protein in the ternary complex of raf, ras-gtp, and kinase on the plasma membrane of living cells. *Journal of Biological Chemistry*, 286(42):36460–36468, 2011.
- D. S. Lidke, F. Huang, J. N. Post, B. Rieger, J. Wilsbacher, J. L. Thomas, J. Pouysségur, T. M. Jovin, and P. Lenormand. Erk nuclear translocation is dimerization-independent but controlled by the rate of phosphorylation. *Journal of Biological Chemistry*, 285(5):3092–3102, 2010.
- NAG. *Numerical Algorithms Group*. d03pl - NAG Toolbox for MATLAB documentation.
- A. Nguyen, W. R. Burack, J. L. Stock, R. Kortum, O. V. Chaika, M. Afkarian, W. J. Muller, K. M. Murphy, D. K. Morrison, R. E. Lewis, J. McNeish, and A. S. Shaw. Kinase suppressor of ras (ksr) is a scaffold which facilitates mitogen-activated protein kinase activation in vivo. *Molecular Cell Biology*, 22(9):3035–3045, 2002.
- I. Novak, P. Kraikivski, and B. Slepchenko. Diffusion in cytoplasm: Effects of excluded volume due to internal membranes and cytoskeletal structures. *Biophysical Journal*, 97:758–767, 2009.
- R. Philips, J. Kondev, and J. Theriot. *Physical biology of the cell*. Garland Science, 2008.
- L. Qiao, R. B. Nachbar, I. G. Kevrekidis, and S. Y. Shvartsman. Bistability and oscillations in the huang-ferrell model of mapk signaling. *PLoS Computational Biology*, 3(9):e184, 09 2007.

- T. Raabe and U. R. Rapp. Ksr—a regulator and scaffold protein of the mapk pathway. *Sci. STKE*, 2002(136):pe28, 2002.
- A. S. Verkman. Solute and macromolecule diffusion in cellular aqueous compartments. *Trends in Biochemical Sciences*, 27(1):27 – 33, 2002.
- M. Weiss, M. Elsner, F. Kartberg, and T. Nilsson. Anomalous subdiffusion is a measure for cytoplasmic crowding in living cells. *Biophysical Journal*, 87(5):3518 – 3524, 2004.
- S. B. Zimmerman and A. P. Minton. Macromolecular crowding: Biochemical, biophysical, and physiological consequences. *Annual Review of Biophysics and Biomolecular Structure*, 22(1):27–65, 1993.